別紙４

研究成果の刊行に関する一覧表レイアウト

書籍

著者氏名	論文タイトル	書籍全体の編集者名	書籍名	出版社名	出版地	出版年	ページ
加藤　健	食道癌 JCOGﾚｼﾞﾒﾝ	有吉　寛	エビデンスに基づいた癌化学療法ハンドブック	メディカルレビュー社	日本	2008	228-233

雑誌

発表者氏名	論文タイトル名	発表誌名	巻号	ページ	出版年
Iriyama T, Takeda K, Shimada Y, et al	ASK1 and ASK2 differentially regulate the counteracting roles of apoptosis and inflammation in tumorigenesis.	The EMBO Journal		1-11	2009
Muto M, Horimatsu T, Ezoe Y, Hori K, Yukawa Y,Morita S,Miyamoto S, Chiba T	Nallow-band imaging of the gastrointestinal tract.	J Gastroenterol.	44	13-25	2009
Ito T, Shimada Y et al	PTTG1 increases cell motility and promotes lymph node metastasis in esophageal squamous cell carcinoma.	Cancer Res	68	3214-3224	2008
Ortiz C, Shimada Y et al.	Gankyrin oncoprotein overexpression as a critical factor for tumor growth in human esophageal squamous cell carcinoma (ESCC) and its clinical significance.	Int J Cancer	122	325-332	2008
Ruike Y, Ichimura A, Tsuchiya S, Shimizu K, Kunimoto R, Okuno Y, Tsujimoto G	Global correlation analysis for micro-RNA and mRNA expression profiles in human cell lines	J Hum Genet	53	515-523	2008
Awakura Y, Nakamura E,Tsujimoto G, et al	Microarray-based identification of CUB-domain containing protein 1 as a potential prognostic marker in conventional renal cell carcinoma.	J Cancer Res Clin Oncol	134	1363-1369	2008

Takahara Y, Kobayashi T, Tsujimoto G, et al.	Phamacogenomics of Cardiovascular Phamacology: Development of an Informatics System for analysis of DNA Microarry Data with a Focus on Lipid Metabolism.	J Pharmacol Sci	107	1-7	2008
Kawanishi H, Matsui Y, Tsujimo G, et al	Secreted CXCL1 is a potential mediator and marker of the tumor invasion of bladder cancer .	Clin Cancer Res	14	2579-2587	2008
Matsui S, Yamanaka T, et al	Clustering of significant genes in prognostic studies with microattays : Application to a clinical study for multiple myeloma.	Statistics in Medicine	27	1106-1120	2008
Mastui S, Shu Zeng, et al	Sample Size Calculations Based on Ranking and Selection in Microarray Experiments	Biometrics	64	217-226	2008
Saito Y, Takisawa H, Kato K,et al	Endoscopic submucosal dissection of recurrent or residual superficial esophageal cancer after chemoradiotherapy.	Gastrointestinal Endoscopy	67	355-359	2008
板坂　聡,et al	食道癌の放射線治療（Radiation Therapy for Esophageal Cancer)	外科治療	99	371-6	2008
加藤　健	特集　食道がんの治療をどう行うか 10.食道がんの分子標的治療の展望	臨床腫瘍プラクティス	5	57-59	2008
波戸岡俊三，篠田雅幸	特集　食道(癌)手術における術中トラブル対処法	手術	62	917-923	2008

Ⅳ. 研究成果の刊行物・別刷

食道癌

A. 保険医療で可能な regimen

FP（5-FU＋CDDP）＋RT 療法（JCOG 9906）

○国立がんセンター中央病院消化器内科　加藤　健

薬剤名（投与方法・投与量）	投与スケジュール（1週）1 2 3 4 5 6 7	（2週）8 9 10 11 12 13 14	（3週）15 16 17 18 19 20 21 ～(日)
CDDP(d.i.v.) 40 mg/m²/day	↓	↓	
5-FU(continuous d.i.v.) 400 mg/m²/day	↓↓↓↓↓	↓↓↓↓↓	
体外照射 2 Gy/day(総量 60 Gy)	↓↓↓↓↓	↓↓↓↓↓	↓↓↓↓↓
granisetron(d.i.v.) 40 μg/kg/day	↑	↑	
dexamethasone(d.i.v.) 20 mg/body/day(Day1), 16 mg/body/day(Day2,3)	↑↑↑		

〈注意〉
腫瘍評価は放射線終了後4週以降に行う。
30 Gy 照射後1週間の予定休止期間をおく。
5週ごと×2コース

〈投与期間〉
化学療法：1週・2週，6週・7週。
放射線治療：1週～3週，6週～8週(15回×2)。

〈保険適応〉
保険適応あり。

奏効例には FP(800/80)×2コース追加

薬剤名（投与方法・投与量）	投与スケジュール 1 2 3 4 5 6 7 8 ・ ・ ・ 28 ～(日)
CDDP(d.i.v.) 80 mg/m²/day	↓
5-FU(continuous d.i.v.) 800 mg/m²/day	↓ ↓ ↓ ↓ ↓
granisetron(d.i.v.) 40 μg/kg/day	↑
dexamethasone(d.i.v.) 20 mg/body/day(Day1), 16 mg/body/day(Day2,3)	↑ ↑ ↑

4週ごと×2コース

治療成績

JCOG 9906 は臨床病期Ⅱ，Ⅲ(T4 を除く)の食道癌を対象とした臨床第Ⅱ相試験である。76 例の患者が登録され，primary endpoint である3年生存率は 47.1％，生存期間中央値は 29 ヵ月，無増悪生存期間は 12 ヵ月，完全奏効率は 62.2％であった。

本療法の特徴

切除可能食道癌の標準的治療は手術，あるいは手術＋術前化学療法であるが，その侵襲は大きく，手術を希望しないあるいは耐術性に問題のある患者に対する治療が求められている。本療法は，そのような患者に対しての標準的治療であり，放射線療法と，放射線増感作用のある 5-FU，CDDP との併用にて治癒が期待できる治療である。同じ対象に対する手術単独療法の成績は，3年生存率で約 50～60％であり，JCOG 9906 の成績と比較すると若干良好であるが，患者背景において，少なからぬ割合で耐術性に問題がある患者が本療法に入っていること，何よりも食道温存可能であるという点を考慮すると，手術に置き換わるほどではないにせよ，十分オプションの1つとして考慮されるべき治療法である。

治療を行っても癌が消失しない場合や，局所に再発した場合には，救済治療として，手術療法や内視鏡的粘膜切除が行われ，長期生存が得られた例も認められる。癌が一旦消失した後もその後1年は3ヵ月ごと，2年目は4ヵ月ごと，3年目以降は6ヵ月ごとにCT，内視鏡によるフォローを行い，再発した場合でも早期に発見し救済することが，重要と考えられている。

主な副作用とその対策

急性期の有害事象と遅発性有害事象の2つに大別される。急性期有害事象では，白血球減少 Grade 4 以上は 1.3 %，好中球減少 Grade 4 以上 1.3 %，血小板減少 Grade 4 以上 0 %と血液毒性は軽微である。非血液毒性は食道炎 Grade 3 以上が 17 %，悪心は Grade 3 以上 17 %，口内炎 Grade 3 以上 8 %，低ナトリウム血症 Grade 3 以上 16 %と，消化器系の毒性が中心である。CDDP は腎障害を来すことから，投与当日ならびにその後数日間 2,000 ～ 3,000 mL/day の補液を必要とする。体重増加に対しては，利尿薬などを用いるが，飲水不十分などで尿量が確保できない場合には，輸液量を調節する。低ナトリウムに陥りやすいため，適度にナトリウムを補充する。

遅発性有害事象は，治療開始数ヵ月後から数年後まで発症することが知られている。放射線の影響が大きいが，胸水 Grade 3 以上が 9 %，Grade 3 以上の食道狭窄や穿孔，嚥下困難などを 13 %，Grade 3 以上の心嚢水貯留を 16 %，Grade 3 以上の放射線肺臓炎を 4 %と無視できない割合で認める。多くの場合ドレナージなどの処置を行うことで改善するが，まれ（5 %）に致死的な経過をたどることがあるため，前もってどのような症状が出現する可能性があるのかなど説明を行い，呼吸困難などの症状が認められた場合には，すぐに対応できるように患者教育を行っておくことも重要である。

EVIDENCE FOR THE REGIMEN

1) Minashi K, et al : ASCO-GI 2008

食道癌

A. 保険医療で可能な regimen

FP（5-FU＋CDDP）＋RT 療法（JCOG 9708，JCOG 9516）

国立がんセンター中央病院消化器内科　加藤　健

薬剤名（投与方法・投与量）	投与スケジュール（1週）1 2 3 4 5 6 7	（2週）8 9 10 11 12 13 14	（3週）15 16 17 18 19 20 21 … 28～(日)
CDDP(d.i.v.) 70 mg/m²/day	↓		
5-FU(continuous d.i.v.) 700 mg/m²/day	↓↓↓↓		
体外照射 2 Gy/day(総量 60 Gy)	↓↓↓↓↓	↓↓↓↓↓	↓↓↓↓↓
granisetron(d.i.v.) 40 μg/kg/day	↑		

（注意）
腫瘍評価は放射線終了後4週以降に行う。
30 Gy 照射後1週間の予定休止期間をおく。

〈投与期間〉
化学療法：1週，5週。
放射線治療：1週～3週，5週～7週(15回×2)。
〈保険適応〉
保険適応あり。

治療成績

JCOG 9708 試験は Stage Ⅰ（T1，N0，M0）食道癌に対する放射線と抗癌剤（CDDP/5-FU）同時併用療法の第Ⅱ相試験である。72 名の患者が登録され，primary endpoint である完全奏効率は 95.8 %であった。2 年生存率は

93.1 %，2 年無病生存率は 75.0 %であった。同対象における標準治療である，手術療法と比しても遜色ない成績が得られた。

JCOG 9516 試験は T 4 あるいは M 1 (LYM) 食道癌症例に対する放射線と抗癌剤同時併用療法の第 II 相試験であり，60 名の患者が登録され，primary endpoint である奏効率は 68.3 %で完全奏効率は 15 %であった。生存期間中央値は 305.5 日と報告されている。同対象は手術療法の適応にならないことが多く，化学放射線療法が標準的治療である。

Stage II，III(nonT 4)に対する本療法の前向き試験の結果は報告されていないが，国立がんセンター中央病院でのレトロスペクティブな検討では，本療法を行った後，奏効例に 5-FU/CDDP 療法(800/80)を 2 コース行った場合の治療成績は完全奏効率 66 %，3 年生存率 48 %と JCOG 9906 とほぼ同等であった。同対象に対しては手術療法，あるいは手術療法＋術前化学療法が標準的治療であるが，本療法も切除可能食道癌患者に対する治療のオプションの 1 つとして考慮されるべきである。

本療法の特徴

JCOG 9906 レジメンと比較して 1 コースの点滴が 4 日間と短縮されているのが特徴である。毒性については大きな差を認めていない。点滴時間が短縮されるというメリットがあるため，プロスペクティブ試験による評価はされていないものの，Stage II，III(nonT 4)食道癌症例に対しても使用されている。対象によって治療成績が異なるため，同じ治療を行う場合でも，対象ごとにリスクベネフィットバランスを考えて行う必要がある。いずれの Stage においても，定期的なフォローアップが重要であることは同様であり，1 年目は 3 ヵ月ごと，2 年目は 4 ヵ月ごと，3 年目以降は 6 ヵ月ごとに CT，内視鏡によるフォローを行い，再発した場合でも早期に発見し救済することが，重要と考えられている。

主な副作用とその対策

JCOG 9708 では，Grade 3 以上の有害事象は白血球減少(8.3 %)，好中球減少 (2.8 %)，血小板減少(1.4 %)，GOT 上昇(1.4 %)，GPT 上昇 (1.4 %) を認めた。JCOG 9516 でもほぼ同等の報告であり，血液毒性，非血液毒性ともに比較的軽微といえる。JCOG 9906 レジメンと同様に，CDDP 投与時には補液を行う必要がある。また，悪心に対しては，予防的にステロイドを Day 1 に 16 ～ 24 mg 使用することで，遅発性の嘔気を押さえることができ，有用である。食道炎は 2 週間後から始まり，Day 29 ～ 36 あたりにピークを迎える。痛みに対してはオピオイドの効果が期待できるため，比較的早期から使用することで，経口摂取量などを増やすことができる。

また，遅発性の有害事象については JCOG 9708 において，Grade 3 の心筋梗塞が 1 例，呼吸困難が 1 例認められている。レトロスペクティブな検討でも，治療開始後の Grade 3 以上の遅発性有害事象発生期間中央値は，肺臓炎は 7.7 ヵ月，心嚢水は 25.7 ヵ月，胸水は 20.4 ヵ月であり，癌の消失後も引き続き注意を払う必要がある。

EVIDENCE FOR THE REGIMEN

1) Kato H, et al : ASCO 2003
2) Ishida K, et al : Jpn J Clin Oncol **34** : 615-619, 2004
3) Takahari D, et al : ASCO-GI 2008

The EMBO Journal (2009), 1–11 | © 2009 European Molecular Biology Organization | All Rights Reserved 0261-4189/09
www.embojournal.org

THE EMBO JOURNAL

ASK1 and ASK2 differentially regulate the counteracting roles of apoptosis and inflammation in tumorigenesis

Takayuki Iriyama[1,9], Kohsuke Takeda[1], Hiromi Nakamura[1], Yoshifumi Morimoto[1], Takumi Kuroiwa[1], Junya Mizukami[1], Tsuyoshi Umeda[1], Takuya Noguchi[1], Isao Naguro[1], Hideki Nishitoh[1], Kaoru Saegusa[1], Kei Tobiume[2], Toshiki Homma[3], Yutaka Shimada[4], Hitoshi Tsuda[5], Satoshi Aiko[6], Issei Imoto[7], Johji Inazawa[7], Kazuhiro Chida[8], Yoshimasa Kamei[9], Shiro Kozuma[9], Yuji Taketani[9], Atsushi Matsuzawa[1] and Hidenori Ichijo[1,*]

[1]Laboratory of Cell Signaling, Graduate School of Pharmaceutical Sciences, The University of Tokyo, CREST, Japan Science and Technology Corporation, and Strategic Approach to Drug Discovery and Development in Pharmaceutical Sciences, Center of Excellence (COE) Program, Bunkyo-ku, Tokyo, Japan, [2]Department of Mucosal Immunology, Hiroshima University Graduate School of Biomedical Sciences, Hiroshima, Japan, [3]Central Research Laboratory, Kissei Pharmaceutical Co. Ltd., Nagano, Japan, [4]Department of Surgery and Science, Graduate School of Medicine and Pharmaceutical Sciences for Research, University of Toyama, Toyama, Japan, [5]Department of Basic Pathology, National Defense Medical College, Saitama, Japan, [6]Department of Surgery, National Defense Medical College, Saitama, Japan, [7]Department of Molecular Cytogenetics, Medical Research Institute and School of Biomedical Science, Tokyo Medical and Dental University, Bunkyo-ku, Tokyo, Japan, [8]Department of Animal Resource Sciences, Graduate School of Agricultural and Life Sciences, The University of Tokyo, Bunkyo-ku, Tokyo, Japan and [9]Department of Obstetrics and Gynecology, Graduate School of Medicine, The University of Tokyo, Bunkyo-ku, Tokyo, Japan

Apoptosis and inflammation generally exert opposite effects on tumorigenesis: apoptosis serves as a barrier to tumour initiation, whereas inflammation promotes tumorigenesis. Although both events are induced by various common stressors, relatively little is known about the stress-induced signalling pathways regulating these events in tumorigenesis. Here, we show that stress-activated MAP3Ks, ASK1 and ASK2, which are involved in cellular responses to various stressors such as reactive oxygen species, differentially regulate the initiation and promotion of tumorigenesis. ASK2 in cooperation with ASK1 functioned as a tumour suppressor by exerting proapoptotic activity in epithelial cells, which was consistent with the reduction in ASK2 expression in human cancer cells and tissues. In contrast, ASK1-dependent cytokine production in inflammatory cells promoted tumorigenesis. Our findings suggest that ASK1 and ASK2 are critically involved in tumorigenesis by differentially regulating apoptosis and inflammation.

The EMBO Journal advance online publication, 12 February 2009; doi:10.1038/emboj.2009.32

Subject Categories: signal transduction; molecular biology of disease

Keywords: apoptosis; ASK1; inflammation; MAP kinase; reactive oxygen species

Introduction

It has been widely recognised that a variety of physicochemical and biological stressors initiates and promotes tumorigenesis (Evan and Vousden, 2001; Murakami *et al*, 2007). Multiple stress-activated signalling systems induce apoptosis in damaged cells, and thereby function as critical defense systems against tumour initiation. On the other hand, such systems are often commonly used as signalling intermediates for inflammation that plays beneficial roles in wound healing and infection. Ironically, however, accumulating evidence has suggested that inflammation, particularly its chronic form, can also be a critical component for tumour promotion (Coussens and Werb, 2002). Therefore, pathophysiological roles of stress-activated signalling systems that regulate apoptosis and inflammation in tumorigenesis have received much attention as therapeutic targets for cancer.

Among the various stress-activated signalling systems, stress-activated mitogen-activated protein (MAP) kinase cascades that converge on c-Jun N-terminal kinases (JNK) and p38 MAP kinases have been characterised as regulators of cellular functions, including apoptosis and inflammation, in response to a wide variety of environmental and biological stressors (Kyriakis and Avruch, 2001). Critical roles of JNK and p38 in tumorigenesis have been revealed recently in mouse models such as those of liver and lung tumorigenesis in p38α-deficient mice (Hui *et al*, 2007; Ventura *et al*, 2007) and skin tumorigenesis in mice deficient in JNK2 or p38-regulated/activated protein kinase (Chen *et al*, 2001; Sun *et al*, 2007). Nevertheless, it has not been fully understood whether and how JNK and p38 regulate apoptosis and inflammation in tumorigenesis.

It has been proposed for decades that oxidative stress triggered by accumulation of reactive oxygen species (ROS) is implicated in tumour initiation and promotion (Benhar *et al*, 2002). ROS production is increased in many types of cancer cells, and elevated ROS levels appear to induce cellular proliferation through constitutive activation of transcription factors such as NF-κB and AP-1 and even induce DNA damage that causes genomic instability, accelerating tumour

*Corresponding author. Laboratory of Cell Signaling, Graduate School of Pharmaceutical Sciences, The University of Tokyo, CREST, Japan Science and Technology Corporation, and Strategic Approach to Drug Discovery and Development in Pharmaceutical Sciences, Center of Excellence (COE) Program, 7-3-1 Hongo, Bunkyo-ku, Tokyo, Japan. Tel.: 81 3 5841 4859; Fax: 81 3 5841 4778;
E-mail: ichijo@mol.f.u-tokyo.ac.jp

Received: 23 August 2008; accepted: 21 January 2009

progression (Hsu *et al*, 2000; Marnett, 2000). In these ROS-medicated oncogenic responses, JNK and p38 have been shown to play multiple roles (Benhar *et al*, 2002; Han and Sun, 2007). Recently, it has been shown that p38α specifically prevents ROS-dependent transforming activity of oncogenic Ras, which not only shows the tumour suppressive role of p38 but also provides indirect evidence of the relevance of ROS in tumorigenesis (Dolado *et al*, 2007). Therefore, ROS-mediated JNK and p38 activation appears to be a key mechanism in stress-associated tumorigenesis.

Activities of JNK and p38 are tightly regulated by their upstream MAP kinase kinases and MAP kinase kinase kinases (MAP3Ks). Among a growing number of MAP3Ks, apoptosis signal-regulating kinase 1 (ASK1) has been widely accepted as a major player in the regulation of ROS-induced JNK and p38 activation (Ichijo *et al*, 1997; Sumbayev and Yasinska, 2005; Takeda *et al*, 2008). ASK1 is preferentially activated by ROS and is required for ROS-induced JNK and p38 activation as well as apoptosis (Tobiume *et al*, 2001). ROS-induced activation of ASK1 is tightly regulated by a redox protein thioredoxin (Trx) and TNF-receptor-associated factors TRAF2 and TRAF6 (Saitoh *et al*, 1998; Tobiume *et al*, 2002; Noguchi *et al*, 2005; Fujino *et al*, 2007). Trx, in its reduced form, binds to ASK1 and inhibits ASK1 activity. In response to ROS, Trx is converted from the reduced form to the oxidised form and dissociates from ASK1. TRAF2 and TRAF6 are then recruited to ASK1 and the activating autophosphorylation of the critical threonine residue in the activation segment of ASK1 is induced. Interestingly, it has been shown recently that ROS-dependent activation of ASK1 also plays a critical role in innate immune responses through production of proinflammatory cytokines in splenocytes and macrophages (Matsuzawa *et al*, 2005). These findings raise the possibility that ASK1 may be involved in apoptosis- and inflammation-related tumorigenesis through ROS-dependent regulation of the JNK and p38 pathways.

As the involvement of ASK1, as well as of other MAP3Ks in the JNK and p38 pathways, in tumorigenesis is largely unknown, we investigated the roles of ASK family kinases, ASK1 and a recently characterised MAP3K, ASK2, in chemically induced skin tumorigenesis in mice, which is an established animal model linking inflammation to tumorigenesis (Mueller, 2006). ASK2 is closely related to ASK1 but can activate the JNK and p38 pathways only by forming a heteromeric complex with ASK1 (Takeda *et al*, 2007). Here, we show that ASK1 and ASK2 are critically involved in tumorigenesis by differentially regulating apoptosis and inflammation in the initiation and promotion stages of tumorigenesis.

Results

ASK2 deficiency promotes chemically induced skin tumorigenesis

To establish an animal model in which we can evaluate the involvement of ASK1 and ASK2 in tumorigenesis, we initially examined the tissue distribution of ASK1 and ASK2 proteins in mice. In contrast to the ubiquitous expression of ASK1, ASK2 protein was highly expressed in the skin as well as the gastrointestinal tract and lung (Figure 1A). ASK2 mRNA was expressed homogeneously throughout the epidermal layer in mouse skin (Figure 1B), and, consistent with this, ASK2 protein was highly expressed in primary keratinocytes derived from the epidermis, compared with macrophagic RAW264.7 cells and primary mouse skin fibroblasts (Figure 1C). We thus explored the possibility of involvement of ASK2 in the development of epidermal tumour using ASK2-deficient ($ASK2^{-/-}$) mice (Supplementary Figure S1).

$ASK2^{-/-}$ mice were viable and fertile and exhibited no apparent abnormalities in the tissues and organs examined including the skin, and no spontaneous tumorigenesis was induced. However, in two-stage skin tumorigenesis experiments, in which the dorsal skin of mice was treated once with DMBA (7,12-dimethylbenz(a)anthracene) and then continually treated with TPA (12-O-tetradecanoylphorbol-13 acetate), papillomas were induced significantly more in $ASK2^{-/-}$ mice than in wild-type (WT) mice (Figure 1D). No difference in the size or histology of papillomas was observed between these mice. The incidence and frequency of papillomas in $ASK2^{+/-}$ mice were intermediate between those in $ASK2^{-/-}$ and WT mice, suggesting that ASK2 gene dosage plays a critical role in tumorigenesis. These results suggested that ASK2 functions as a tumour suppressor in the skin.

ASK2 functions as a tumour suppressor by facilitating DMBA-induced apoptosis in epidermal keratinocytes

To investigate the possible involvement of ASK2 in DMBA-induced tumour initiation, we examined whether DMBA activates ASK2 by immunoblotting using phospho-ASK antibody, that specifically recognises the activating phosphorylation of the critical threonine residue conserved between ASK1 and ASK2 (Tobiume *et al*, 2002). Consistent with the previous finding that ASK2 exhibited responsiveness to oxidative stress such as H_2O_2 only by forming a complex with ASK1 (Takeda *et al*, 2007), DMBA-induced activating phosphorylation of ASK2 was induced in HEK293 cells co-expressing ASK2 and kinase-negative mutant of ASK1 (ASK1-KN), but not in those expressing only ASK2 (Figure 2A). Moreover, reactiveness to phospho-ASK antibody (p-ASK1/2) increased in response to DMBA in primary keratinocytes derived from WT mice, which was strongly reduced in those derived from $ASK2^{-/-}$ mice (Figure 2B), indicating that ASK2, probably as well as ASK1, was activated by treatment with DMBA. Importantly, DMBA-induced activation of JNK and p38 was also reduced in $ASK2^{-/-}$ primary keratinocytes, compared with WT keratinocytes (Figure 2B). These results suggested that the ASK2-JNK and -p38 pathways are activated by DMBA in keratinocytes.

In the initiation stage in two-stage skin tumorigenesis, elimination of cells severely damaged by DMBA, so called 'initiated' cells, is a prerequisite for tumour suppression. Given that ASK2 in a complex with ASK1 had potential to induce apoptosis (Takeda *et al*, 2007), we expected that ASK2 contributed to DMBA-induced apoptosis in keratinocytes. Whereas no significant differences were observed between the viability of WT and $ASK2^{-/-}$ keratinocytes in the absence of DMBA treatment, $ASK2^{-/-}$ cells were more resistant to the toxic effects of DMBA than WT cells (Figure 2C). We also found that DMBA-induced DNA fragmentation was significantly reduced in $ASK2^{-/-}$ keratinocytes, compared with WT cells (Figure 2D). These results suggested that ASK2 is required for DMBA-induced apoptosis at least in primary keratinocytes.

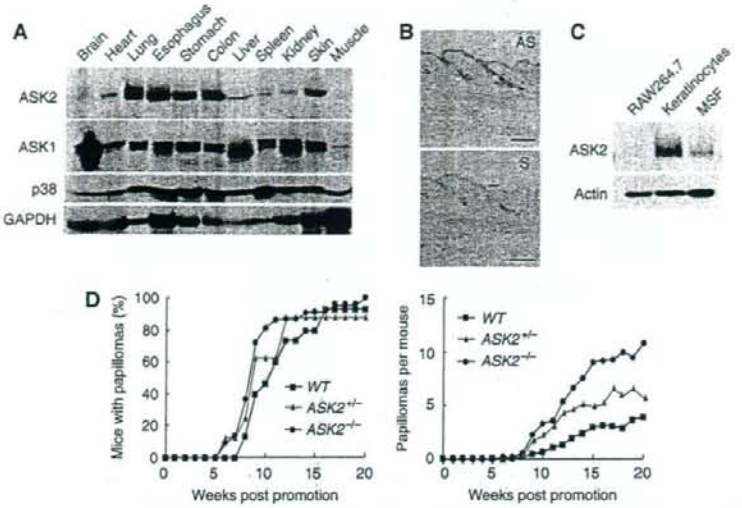

Figure 1 ASK2 deficiency promotes chemically induced skin tumorigenesis. (**A**) Normal tissue distribution of ASK2 in mice. Cell lysates were obtained from the indicated mouse organs and levels of protein expression of ASK1 and ASK2 were detected by immunoblotting. (**B**) Expression of ASK2 mRNA in mouse skin. ASK2 mRNA was detected by *in situ* hybridisation of adult mouse skin with anti-sense (AS) and sense (S) riboprobes. Scale bar = 100 μm. (**C**) ASK2 protein is highly expressed in primary keratinocytes. ASK2 protein was detected by immunoblotting in various cultured mouse cells. RAW264.7, a macrophagic cell line; Keratinocytes, primary keratinocytes; MSF, mouse skin fibroblasts. (**D**) Chemically induced skin tumorigenesis is promoted in $ASK2^{-/-}$ mice. Wild-type (WT; $n = 15$), $ASK2^{-/-}$ ($n = 7$) and $ASK2^{-/-}$ mice ($n = 22$) were treated once with DMBA (100 μg in 200 μl of acetone) and then continually treated with TPA (10 μg in 200 μl of acetone) twice a week for 20 weeks. The percentage of mice with papillomas (left) and the average number of papillomas per mouse (right) are shown.

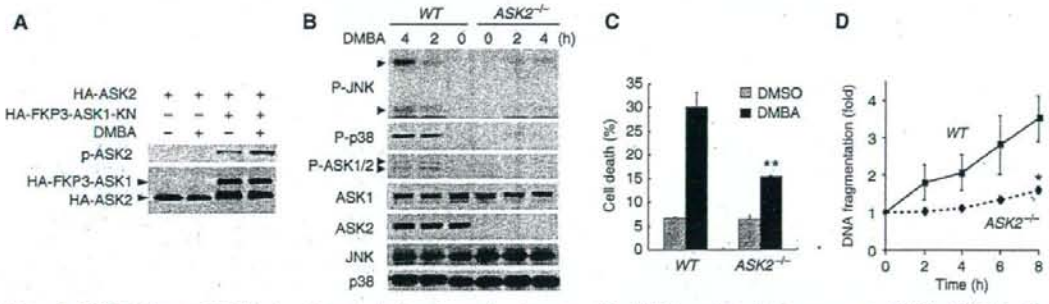

Figure 2 ASK2 facilitates DMBA-induced apoptosis in primary keratinocytes. (**A**) ASK2 is activated in response to DMBA. HEK293 cells transfected with HA-ASK2 in combination with (+) or without (−) HA-FKP3-ASK1-kinase-negative (KN) were treated (+) or not (−) with 100 μM DMBA for 1 h. Cell lysates were subjected to immunoblotting. (**B**) Immunoblotting of primary keratinocytes treated with 100 μM DMBA for the indicated periods. Phospho-ASK antibody recognised activation states of both ASK1 and ASK2 (p-ASK1/2). (**C**) $ASK2^{-/-}$ primary keratinocytes were more resistant to the toxic effects of DMBA than WT cells. WT and $ASK2^{-/-}$ keratinocytes were treated with DMSO or 100 μM DMBA for 8 h. Live and dead cells were simultaneously stained with 0.5 mM calcein AM and 0.5 mM EthD-1, respectively. Percentage of dead cells (at least 200 cells were counted for each group) is shown. Data are mean ± s.e.m. ($n = 3$). $^{**}P < 0.01$, compared with DMBA-treated WT cells. (**D**) DMBA-induced apoptosis is suppressed in $ASK2^{-/-}$ primary keratinocytes. DNA fragmentation in WT and $ASK2^{-/-}$ primary keratinocytes treated with 100 μM DMBA for the indicated periods was quantified. Data are presented as the fold increases relative to the value of unstimulated cells and are mean ± s.e.m. ($n = 3$). $^{*}P < 0.05$, compared with WT cells treated with DMBA for 8 h.

To examine whether ASK2 is indeed required for DMBA-induced apoptosis in epidermal cells *in vivo*, apoptotic cells in the DMBA-treated dorsal skin were detected by staining for active caspase-3 and TUNEL. Both active caspase-3-positive and TUNEL-positive cells were fewer in number in $ASK2^{-/-}$ mice than in WT mice (Figure 3). On the other hand, there was no obvious difference in proliferation of epidermal keratinocytes, as assessed by Ki67 staining, between WT and $ASK2^{-/-}$ mice treated with DMBA and/or TPA (Supplementary Figures S2). Taken together with the finding that the TPA-induced inflammation in $ASK2^{-/-}$ skin was comparable to that in WT skin (see below), these results suggested that ASK2 primarily functions, through its proapoptotic activity, as a tumour suppressor by eliminating damaged keratinocytes in the initiation stage.

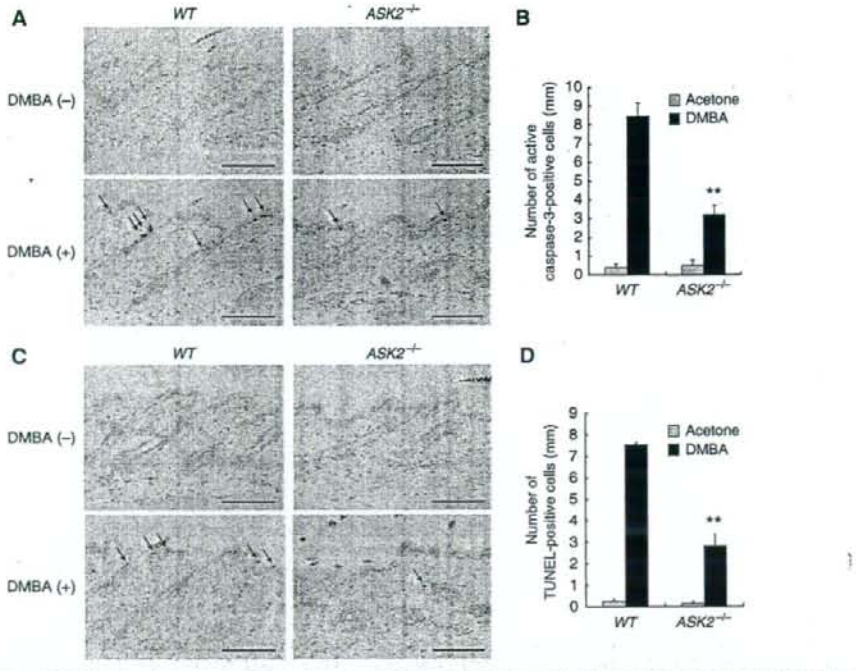

Figure 3 ASK2 facilitates DMBA-induced apoptosis in the epidermis. (**A**) Immunohistochemical staining of DMBA-treated skin sections with an antibody against active caspase-3. Skin samples were taken 24 h after the application of acetone (DMBA (−)) or 100 μg DMBA. Images are representatives of three independent experiments. Arrows indicate active caspase-3-positive cells. Scale bar = 100 μm. (**B**) Quantification of active caspase-3-positive cells. The number of active caspase-3-positive cells in the hair follicles and interfollicular epidermis was counted over a linear distance of approximately 15 mm, and averaged for each 1-mm interval. Values are the mean ± s.e.m. ($n = 3$). $^{**}P < 0.01$, compared with DMBA-treated WT mice. (**C**) TUNEL staining of sections as in (A). Arrows indicate TUNEL-positive cells. Scale bar = 100 μm. (**D**) Quantification of TUNEL-positive cells. The number of TUNEL-positive cells was counted and averaged as in (B). Values are the mean ± s.e.m. ($n = 3$). $^{**}P < 0.01$, compared with DMBA-treated WT mice.

ASK2 is critically involved in the signalling evoked by ROS-producing carcinogenic stimuli

DMBA is metabolised to toxic metabolites and ROS, the latter of which causes oxidative DNA damage in the skin (Frenkel *et al*, 1995; Muqbil *et al*, 2006). We found that ROS were indeed produced by DMBA treatment in human HaCaT keratinocytes, which was significantly inhibited by antioxidants *N*-acetyl-L-cysteine and propyl gallate (PG) (Figure 4A). Importantly, DMBA-induced ASK2 activation was inhibited by PG in HEK293 cells stably co-expressing ASK2 and ASK1-KN (293-ASK2/1KN cells), indicating that ROS were involved in DMBA-induced ASK2 activation (Figure 4B). Consistent with this finding, DMBA-induced activation of endogenous JNK, p38 and ASK2, as well as ASK1, was also inhibited by antioxidants in keratinocytes (Figure 4C). As DMBA-induced ROS production itself was not attenuated in the absence of ASK2 (Supplementary Figure S3), and ASK2 was required for ROS-induced JNK and p38 activation in keratinocytes (Supplementary Figure S4), ROS produced by DMBA appeared to activate the ASK2-JNK/p38 cascades. We also found that antioxidants significantly reduced DMBA-induced apoptosis in WT keratinocytes (Figure 4D). These findings indicated that ROS played a key role in ASK2-dependent apoptosis in DMBA-treated keratinocytes.

We next examined the involvement of ASK2 in ultraviolet (UV) response as a more physiologically relevant stimulant of human carcinogenesis. UV is classified into three types based on wavelengths, UVA (320–400 nm), UVB (290–320 nm) and UVC (200–290 nm). Among these, UVA reaches the earth's surface and is, therefore, a major skin carcinogen (Agar *et al*, 2004). As has been reported previously (Valencia and Kochevar, 2006), UVA, but not UVC, induced ROS production in HaCaT cells (Supplementary Figure S5A). Physiologically relevant doses of UVA was used in this and latter experiments (Bode and Dong, 2003). In 293-ASK2/1KN cells, ASK2 was strongly activated by UVA, but to a lesser extent by UVC, in a time- and dose-dependent fashion (Supplementary Figure S5B). Although UVB is also known as a strong skin carcinogen, UVA was a stronger activator of ASK2 than UVB, at least in our assay system. Pretreatment with the antioxidants suppressed the UVA-induced activation of ASK2 in 293-ASK2/1KN cells (Figure 4E), indicating that ASK2 was activated in response to ROS induced by UVA. Moreover, UVA-induced activation of JNK and p38 was reduced in *ASK2*$^{-/-}$ keratinocytes (Figure 4F). We also found that *ASK2*$^{-/-}$ keratinocytes were more resistant to UVA-induced cell death than WT cells (Figure 4G). These results suggested that ASK2 widely plays a proapoptotic role in response to ROS-producing carcinogenic stimuli.

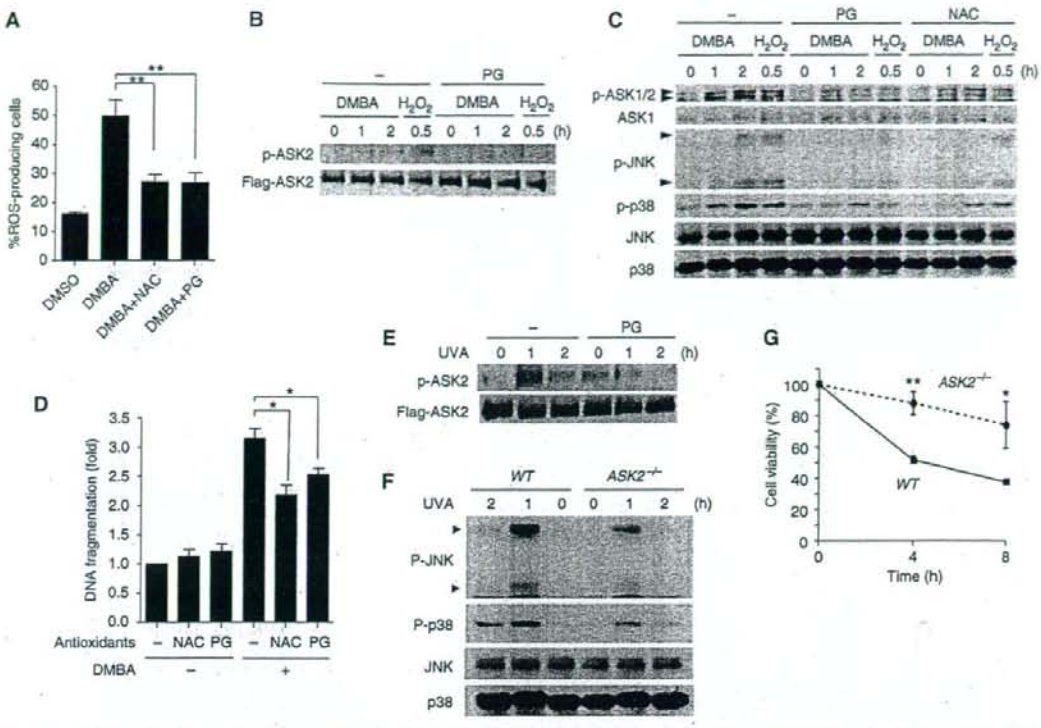

Figure 4 ASK2 is critically involved in the signalling evoked by ROS-producing carcinogenic stimuli. (**A**) DMBA induces intracellular ROS production. HaCaT cells were pretreated with 1 mM *N*-acetylcysteine (NAC) or 20 μM propyl gallate (PG) for 15 min and then stimulated with DMSO or 100 μM DMBA for 30 min. ROS production was measured by FACS analysis and the percentage of ROS-producing cells was calculated. Values are the mean ± s.e.m. ($n = 5$). $^{**}P < 0.01$. (**B**) DMBA-induced activation of ASK2 is inhibited by antioxidants. 293-ASK2/1KN cells were pretreated with (+) or without (−) 20 μM PG for 15 min and then stimulated with 100 μM DMBA or 0.3 mM H_2O_2. Cell lysates were subjected to immunoblotting. (**C**) Immunoblotting of WT primary keratinocytes pretreated with antioxidants (20 μM PG or 1 mM NAC) for 15 min and stimulated with 100 μM DMBA or 0.3 mM H_2O_2 for the indicated periods. (**D**) DMBA-induced apoptosis in primary keratinocytes is reduced by antioxidants. DNA fragmentation in WT primary keratinocytes pretreated with 20 μM PG or 1 mM NAC for 15 min and stimulated with (+) or without (−) 100 μM DMBA for 8 h. Data are presented as the fold increases relative to the value of untreated cells and are mean ± s.e.m. ($n = 4$). $^{*}P < 0.05$. (**E**) UVA-induced activation of ASK2 is mediated by ROS. 293-ASK2/1KN cells were pretreated with (+) or without (−) 20 μM PG for 15 min and then stimulated with 80 kJ/m^2 UVA for the indicated periods. Cell lysates were subjected to immunoblotting. (**F**) UVA-induced activation of JNK and p38 is reduced in *ASK2*$^{-/-}$ primary keratinocytes. WT and *ASK2*$^{-/-}$ primary keratinocytes were treated with 80 kJ/m^2 UVA for the indicated periods. Cell lysates were subjected to immunoblotting. (**G**) UVA-induced cell death is reduced in *ASK2*$^{-/-}$ primary keratinocytes. Viability of WT and *ASK2*$^{-/-}$ primary keratinocytes treated with 80 kJ/m^2 UVA was measured by MTT assay. Data are presented as the percentage of viable cells and are mean ± s.e.m. ($n = 3$). $^{*}P < 0.05$, $^{**}P < 0.01$, compared with WT cells.

ASK2 appears to function as a tumour suppressor in human epithelial cancers

To explore the roles of ASK2 in human carcinogenesis, we examined ASK2 expression in various human cancer cells and tissues. In contrast to cervical and ovarian cancer cell lines, in which mRNA expression of ASK2 was inconsistent and varied, ASK2 expression was reduced in many cancer cell lines derived from the gastrointestinal tract (Figure 5A). In representative cell lines derived from esophageal cancer (KYSE30, KYSE110, KYSE850 and KYSE1250 cells), levels of expression of ASK2 mRNA were correlated well with those of ASK2 protein (Figure 5B). Immunohistochemical analysis of esophageal squamous cell carcinoma (ESCC) specimens revealed that ASK2 level was indeed reduced in 46 of 100 cases examined (Figure 5C). Moreover, a specimen of the boundary of the normal tissue and ESCC in an ASK2-negative case clearly showed that ASK2 protein was specifically reduced in ESCC (Figure 5D). These findings together suggested that ASK2 functions as a tumour suppressor in human epithelial cancers.

Tumour-promoting activity of ASK1 counteracts with the proapoptotic activity of ASK1 and ASK2 in keratinocytes

The stability and activity of ASK2 protein are preserved only with formation of a heteromeric complex with ASK1 (Takeda *et al*, 2007). As ASK2 expression was strongly reduced in *ASK1*$^{-/-}$ keratinocytes (Figure 6A), it is possible that *ASK1*$^{-/-}$ mice are also prone to skin tumorigenesis. This was supported by the findings that DMBA-induced JNK and p38 activation was inhibited in *ASK1*$^{-/-}$ keratinocytes (Figure 6A) and that DMBA-induced apoptosis in *ASK1*$^{-/-}$ keratinocytes was suppressed to a level similar to that in *ASK2*$^{-/-}$ cells (Figure 6B). Intriguingly, however, no major

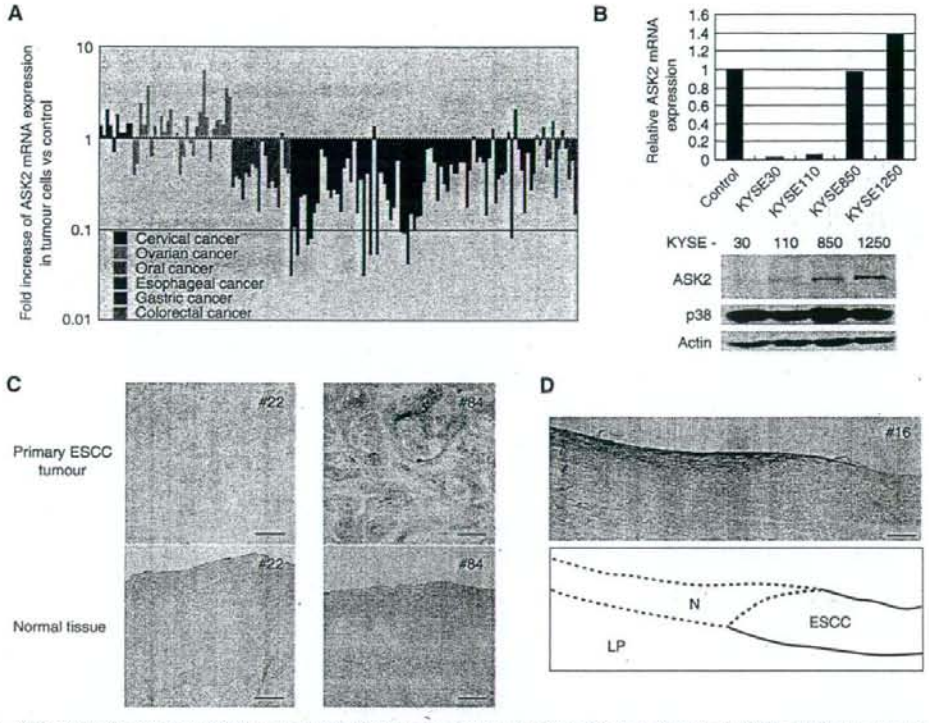

Figure 5 ASK2 expression is reduced in human cancer cell lines and tissues. (**A**) Quantification of levels of ASK2 mRNA expression in various human cancer cell lines. Real-time RT–PCR of ASK2 mRNA in cancer cell lines and respective normal tissues was carried out. After normalisation to GAPDH, levels of ASK2 mRNA expression in each human cancer cell line are indicated as fold increase relative to that in the respective normal tissue. (**B**) mRNA and protein expression of ASK2 in esophageal cancer cell lines, KYSE30, KYSE110, KYSE850 and KYSE1250. Data of mRNA expression of ASK2 was extracted from Figure 5A. Protein expression of ASK2 was detected by immunoblotting. (**C, D**) Immunohistochemical staining of ASK2 protein in esophageal cancer specimens. Representative ASK2-negative (#22) and ASK2-positive (#84) cases are shown in (C). The boundary of the normal tissue (N) and ESCC in an ASK2-negative case (#16) is shown in (D). LP, lamina propria. Scale bar = 100 μm.

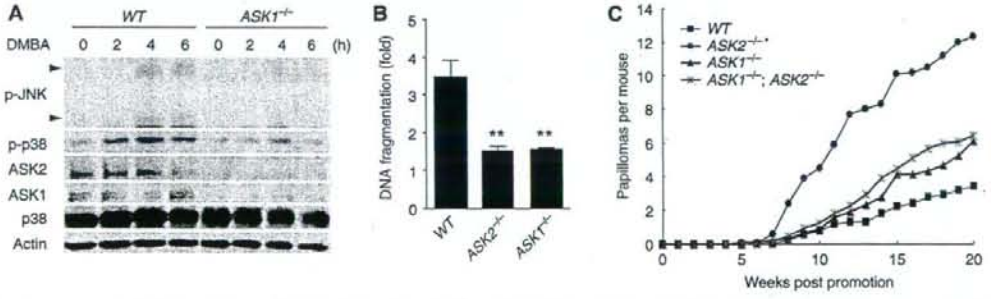

Figure 6 Tumour-promoting activity of ASK1 counteracts with the proapoptotic activity of ASK1 and ASK2 in keratinocytes. (**A**) DMBA-induced activation of JNK and p38 is reduced in *ASK1*$^{-/-}$ primary keratinocytes. Immunoblotting of WT and *ASK1*$^{-/-}$ primary keratinocytes treated with 100 μM DMBA for the indicated periods. (**B**) DMBA-induced apoptosis is suppressed in *ASK1*$^{-/-}$ primary keratinocytes to a similar level to that in *ASK2*$^{-/-}$ cells. DNA fragmentation in WT, *ASK1*$^{-/-}$ and *ASK2*$^{-/-}$ primary keratinocytes treated with 100 μM DMBA for 8 h was quantified. Data are presented as the fold increases relative to the value of respective unstimulated cells and are mean ± s.e.m. ($n = 4$). **$P < 0.01$, compared with WT cells. (**C**) Two-stage skin tumorigenesis induced by DMBA and TPA in WT ($n = 14$), *ASK2*$^{-/-}$ ($n = 10$), *ASK1*$^{-/-}$ ($n = 9$) and *ASK1*$^{-/-}$; *ASK2*$^{-/-}$ ($n = 11$) mice. The average number of papillomas per mouse is shown.

increase in skin tumorigenesis was observed in *ASK1*$^{-/-}$ mice (Figure 6C). More convincingly, mice deficient in ASK1 and ASK2 (*ASK1*$^{-/-}$; *ASK2*$^{-/-}$ mice) exhibited an extent of tumorigenesis similar to that in *ASK1*$^{-/-}$ mice (Figure 6C), suggesting that ASK1 is required for the increased tumorigenesis in *ASK2*$^{-/-}$ mice. Thus, ASK1 appeared to play two

opposite roles in skin tumorigenesis: a tumour suppressive function in cooperation with ASK2 and a tumour promoting function independent of ASK2.

ASK1-dependent inflammatory response is required for tumour promotion

Therefore, we examined whether and how ASK1 and ASK2 contribute to TPA-dependent tumour promotion. TPA is recognised as the most potent tumour promoter, which induces pleiotrophic tissue response encompassing a strong inflammatory reaction, leading to the proliferation of initiated cells (Mueller, 2006). After topical treatment of the dorsal skin with TPA, the epidermis of WT and *ASK2*$^{-/-}$ mice exhibited dramatic hyperplasia with extensive infiltration of inflammatory cells, whereas the epidermis of *ASK1*$^{-/-}$ mice exhibited considerably milder hyperplasia (Figure 7A). This was supported by the significant difference in epidermal thickness between WT or *ASK2*$^{-/-}$ mice and *ASK1*$^{-/-}$ mice treated with TPA (see the graph in Figure 7A). Proliferation of basal keratinocytes in *ASK1*$^{-/-}$ and *ASK1*$^{-/-}$; *ASK2*$^{-/-}$ mice was less prominent than that in WT and *ASK2*$^{-/-}$ mice (Supplementary Figure S6). Moreover, p38 activation was not induced in TPA-treated *ASK1*$^{-/-}$ skin (Figure 7B). Consistent with the well-established roles of p38 in cytokine production (O'Neill, 2006) and the requirement of proinflammatory cytokines such as TNF-α and IL-6 for chemically induced skin tumorigenesis (Moore *et al*, 1999; Suganuma *et al*, 1999; Ancrile *et al*, 2007), we found that TPA-induced production of TNF-α and IL-6 was diminished in the skin of *ASK1*$^{-/-}$ and *ASK1*$^{-/-}$; *ASK2*$^{-/-}$ mice (Figure 7C) and also in papillomas extirpated from *ASK1*$^{-/-}$ mice (Supplementary Figure S7). These results suggested that ASK1, but not ASK2, played a critical role in TPA-induced inflammation, at least in part through cytokine production.

Continual application of TPA to the skin is known to induce excess production of ROS (Nakamura *et al*, 1998; Ha *et al*, 2006). Thus, we expected that ASK1 regulated TPA-induced inflammation in a ROS-dependent fashion and that the cells, in which ASK1, but not ASK2, was required for ROS-induced cellular responses, played a critical role in TPA-

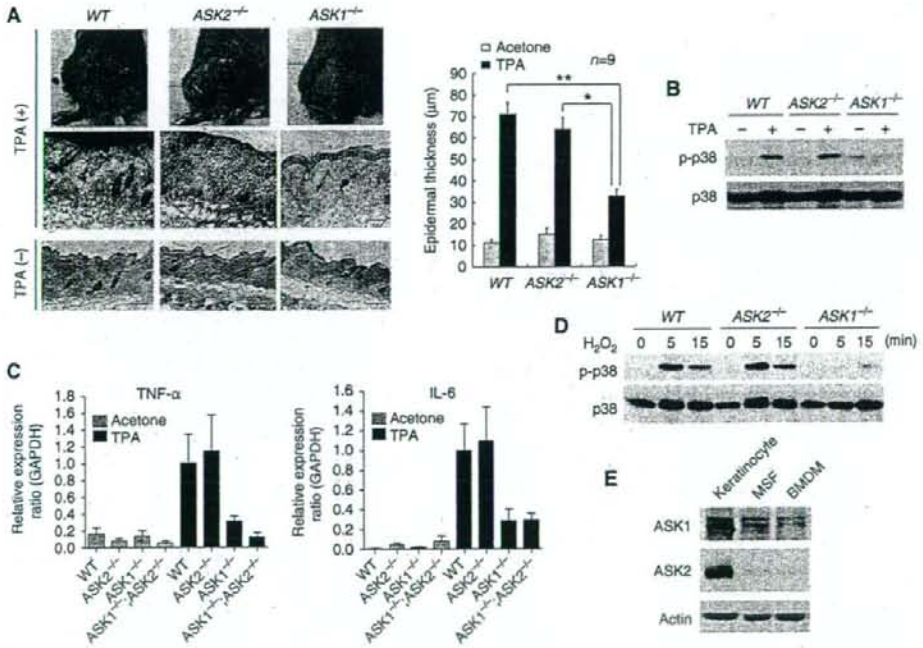

Figure 7 ASK1-dependent inflammatory response is required for tumour promotion. (**A**) TPA-induced inflammatory response is reduced in *ASK1*$^{-/-}$ mice. The dorsal skin of WT, *ASK2*$^{-/-}$ and *ASK1*$^{-/-}$ mice was treated twice with acetone (TPA (−)) or TPA (10 μg each) with 24 h interval. Mice were killed 48 h after the latter treatment, and skin sections were processed for hematoxylin-eosin staining. Images are representatives of nine mice for each genotype. Scale bar = 100 μm. Macroscopic observations of the dorsal skin of TPA-treated mice are also shown (left top panels). Quantification of epidermal thickness of these mice is shown in a graph on the right. Values are the mean ± s.e.m. ($n = 9$). $^{*}P<0.05$, $^{**}P<0.01$, compared with TPA-treated WT mice. (**B**) TPA-induced activation of p38 is attenuated in *ASK1*$^{-/-}$ skin. Acetone and 10 μg TPA were independently applied to separate areas of the dorsal skin of the same mouse. Mice were killed at 24 h after treatment, and each treated region of skin was excised and lysed and then subjected to immunoblotting. (**C**) Induction of TNF-α and IL-6 is attenuated in TPA-treated skin of *ASK1*$^{-/-}$ and *ASK1*$^{-/-}$;*ASK2*$^{-/-}$ mice. The dorsal skin of WT, *ASK2*$^{-/-}$, *ASK1*$^{-/-}$ and *ASK1*$^{-/-}$;*ASK2*$^{-/-}$ mice was treated with acetone or 10 μg TPA. Mice were killed 24 h after the treatment, and RNA was extracted from the treated skin. mRNA expression of TNF-α and IL-6 was quantified using real-time RT–PCR. Data are mean ± s.e.m. ($n = 4$ for TPA-treated mice and $n = 3$ for acetone-treated mice). (**D**) H_2O_2-induced activation of p38 is reduced in bone marrow-derived macrophages (BMDMs) from *ASK1*$^{-/-}$ mice, but not from *ASK2*$^{-/-}$ mice. WT, *ASK2*$^{-/-}$ and *ASK1*$^{-/-}$ BMDM were treated with 0.3 mM H_2O_2 for the indicated periods. Cell lysates were subjected to immunoblotting. (**E**) Comparison of ASK1 and ASK2 protein expression among primary cultured mouse cells. Cell lysates from primary keratinocytes, mouse skin fibroblasts (MSF) and BMDM were subjected to immunoblotting.

induced inflammation. Reductions in H_2O_2-induced p38 activation in both *ASK1*$^{-/-}$ and *ASK2*$^{-/-}$ keratinocytes indicated the similar roles of ASK1 and ASK2 in response to ROS in keratinocytes (Supplementary Figure S4), suggesting that ASK1 exerts its specific function in TPA response in other cell types than keratinocytes. This hypothesis, together with the ROS-dependent requirement of ASK1 for lipopolysaccharide (LPS)-induced p38 activation and cytokine production in splenocytes and macrophages (Matsuzawa *et al*, 2005), raised the possibility that ASK1 was selectively required for cytokine production in inflammatory cells. In fact, ROS-induced p38 activation was reduced in bone marrow-derived macrophages (BMDMs) from *ASK1*$^{-/-}$ mice, but not from *ASK2*$^{-/-}$ mice (Figure 7D). Consistent with this, ASK2 expression was much lower in BMDMs than in keratinocytes, whereas similar levels of ASK1 were expressed in these cells (Figure 7E). These findings suggested that, in inflammatory cells such as macrophages, ASK1 contributed to TPA-induced inflammatory response, which was found to be a prerequisite for promotion of skin tumorigenesis.

Discussion

In this study, our findings provide evidence for novel functions of stress-activated MAP3Ks in tumorigenesis (Figure 8). Proapoptotic activity of ASK2 in cooperation with ASK1 in epithelial cells and ASK1-dependent cytokine production in inflammatory cells were found to be critical determinants of chemically induced skin tumorigenesis in mice. Intriguingly, ROS appear to play critical roles in the regulation of the ASK family kinases in both these tumour-suppressing and tumour-promoting processes.

ASK2 is a recently identified MAP3K that interacts with ASK1, but functions of ASK2 have not been well understood, except that it activates the JNK and p38 pathways, induces apoptosis, and is required for ROS-induced activation of JNK (Takeda *et al*, 2007). By the two-stage skin tumorigenesis experiment using *ASK2*$^{-/-}$ mice, ASK2 was found to function as a tumour suppressor primarily by inducing apoptosis in epidermal keratinocytes in the initiation stage. Here, we propose that this function of ASK2 is also relevant to human cancers, as expression of ASK2 was strongly reduced in various human gastrointestinal cancer cells and tissues compared with their normal counterparts. This reduced ASK2 expression may be related, in part, to the fact that the human

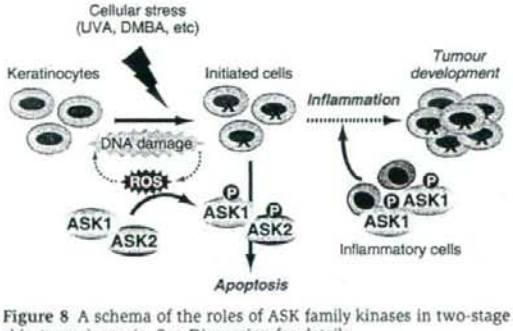

Figure 8 A schema of the roles of ASK family kinases in two-stage skin tumorigenesis. See Discussion for details.

ASK2 gene is located on chromosome 1p36.1, a region that is frequently deleted in a variety of human tumours (Kaghad *et al*, 1997).

As the stability and activity of ASK2 protein is preserved only with formation of a heteromeric complex with ASK1 (Takeda *et al*, 2007), proapoptotic activity of ASK2 in keratinocytes appeared to depend on ASK1. In fact, DMBA-induced apoptosis in *ASK1*$^{-/-}$ keratinocytes was reduced to a similar extent to that in *ASK2*$^{-/-}$ keratinocytes (Figure 6B), suggesting that ASK1 functions cooperatively with ASK2 in DMBA-induced apoptosis in keratinocytes. The finding that reactiveness to phospho-ASK antibody was abolished in DMBA-treated *ASK2*$^{-/-}$ keratinocytes, even though ASK1 protein still existed (Figure 2B), also suggests the cooperative regulation of activity of ASK1 and ASK2. This cooperation may be accounted for by the previous finding that ASK1 and ASK2 in their heteromeric complex activated each other not only by stabilisation of ASK2 by ASK1, but also by direct activating phosphorylation of ASK1 by ASK2 (Takeda *et al*, 2007).

Proapoptotic activity of ASK2 was found to be evoked by ROS production upon DMBA, although the source of ROS has not been specified. In *ASK2*$^{-/-}$ keratinocytes, DMBA-induced activation of JNK and p38 was reduced, suggesting that ASK2, as well as ASK1, has an important function in the regulation of ROS-induced JNK and p38 activation. Taken together with the accumulating evidence suggesting the multiple roles of JNK and p38 in ROS-medicated oncogenic responses (Benhar *et al*, 2002; Han and Sun, 2007), the ROS-activated ASK1–ASK2 complex appears to exert its proapoptotic activity through the JNK and/or p38 pathways. However, the underlying mechanism by which JNK and p38 induce apoptosis in DMBA-treated keratinocytes has not been elucidated so far. Considering the recent understandings that JNK and p38 exhibit pro- or anti-apoptotic activity depending on cell type and cellular context (Liu and Lin, 2005; Zarubin and Han, 2005), JNK and p38 may be required, but not sufficient, components for DMBA-induced apoptosis in keratinocytes. Critical roles of ASK2 in the signalling evoked by ROS-producing carcinogenic stimuli was also suggested by the findings that ASK2 was activated by UVA in a ROS-dependent fashion and that ASK2 was required for UVA-induced cell death. Given that UVA is regarded as a physiologically relevant stimulant of human carcinogenesis, we propose again that ASK2 may be a tumour suppressor in humans.

Compared with ASK2, the roles of ASK1 in tumorigenesis are more divergent. ASK1 exerts tumour-suppressive activity in cooperation with ASK2 in the initiation stage, whereas ASK1 accelerates tumorigenesis by facilitating production of inflammatory cytokines such as TNF-α and IL-6 in the promotion stage (Figure 8). Mice deficient in these cytokines have been shown to be resistant to two-stage skin tumorigenesis, supporting our hypothesis (Moore *et al*, 1999; Suganuma *et al*, 1999; Ancrile *et al*, 2007). The predominant expression of ASK1 in inflammatory cells such as BMDMs appears to be a plausible explanation for the fact that the proinflammatory role was assigned specifically to ASK1, but not to ASK2. Importantly, it has been shown recently that ASK1 mediates LPS-induced p38 activation and cytokine production in a ROS-dependent fashion in splenocytes and macrophages (Matsuzawa *et al*, 2005), showing the critical role of ASK1 in innate immunity. Taking into account

evidence suggesting that excess ROS are produced upon continual treatment of the skin with TPA (Nakamura *et al*, 1998; Ha *et al*, 2006), the ROS-mediated ASK1-p38 pathway, which otherwise plays a beneficial role as a host defense system against pathogen, may play an adverse role in inflammation-induced tumorigenesis.

In addition to the skin, ASK2 is highly expressed in the gastrointestinal tract and lung, which are constantly exposed to a variety of stress stimuli such as toxic agents and invading pathogens from external environments. In these organs, correlation between inflammation, particularly chronic inflammation, and cancer has been established (Azad *et al*, 2008; Roessner *et al*, 2008). For instance, *Helicobacter pylori* gastritis and inflammatory bowel disease increase risks of developing gastric and colorectal cancers, respectively, and inflammation induced by cigarette smoke and ambient air pollutants is a major risk factor of lung cancer. Under such inflammatory conditions, inflammatory cells such as neutrophils and macrophages produce large amounts of ROS, which further enhance inflammation in part through upregulation of proinflammatory cytokines and predispose cells to malignant transformation. In this regard, proapoptotic function of ASK2 in cooperation with ASK1 in epithelial cells and proinflammatory function of ASK1 in inflammatory cells may also be involved in inflammation-related carcinogenesis in the gastrointestinal tract and lung.

In conclusion, genetic findings in this study strongly suggest that ASK1- and ASK2-dependent apoptosis of keratinocytes in the initiation stage and ASK1-dependent cytokine production in inflammatory cells in the promotion stage are critical steps in tumorigenesis. These stage- and cell type-dependent counteracting functions of stress-activated MAP kinase pathways thus appear to be critical determinants of apoptosis- and inflammation-related carcinogenesis and may have implications for cancer prevention and treatment.

Materials and methods

Mice

Generation of mice deficient for the *ASK1 (MAP3K5)* gene has been described (Tobiume *et al*, 2001). The 6.5 and 1.5 kb fragments of the *ASK2 (MAP3K6)* gene were used as homologous regions for recombination. pBluescript SK (Stratagene) was used as a backbone to construct the targeting vector with a DT-A cassette for negative selection. The first (3′ of the initiation codon) to fifth exons were replaced by NLS-LacZ (coding sequence for β-galactosidase containing nuclear localisation signal sequence followed by poly A signal) and a reverse-oriented PGK-neo cassette. The linearised targeting vector was electroporated into E14 ES cells. G418-resistant ES clones with the intended recombination were screened by Southern blot analysis. Heterozygous mutant ES cells were injected into C57BL/6J blastocysts. Germline transmission of mutated alleles to F1 mice obtained by intercross of resultant male chimeras and female C57BL/6J was confirmed by Southern blot analysis. Homozygous mutant mice were obtained by F1 heterozygous intercrosses. Deficiency of ASK2 polypeptide was confirmed by immunoblot analysis. *ASK1*$^{-/-}$ and *ASK2*$^{-/-}$ mice were backcrossed onto the C57BL/6J strain for 12 and 10 generations, respectively. All experiments accorded with protocols approved by the Animal Research Committee of the Graduate School of Pharmaceutical Sciences, The University of Tokyo (Tokyo, Japan).

Two-stage skin tumorigenesis model

The dorsal skin of 8–9-week-old female mice was treated once with DMBA (100 μg in 200 μl of acetone). One week later, it was continually treated with TPA (10 μg in 200 μl of acetone) twice a week for 20 weeks.

Cell culture, antibodies and reagents

See Supplementary information.

Expression plasmids and transfection

Epitope-tagged mammalian expression plasmids for ASK1 and ASK2 were described previously (Takeda *et al*, 2007). Transfection of these expression plasmids into HEK293 cells was performed with FuGENE 6 (Roche Applied Science) according to the manufacturer's instructions.

In situ hybridisation

For generation of anti-sense and sense RNA probes, a 429 bp DNA fragment corresponding to nucleotide positions 697–1125 of mouse ASK2 (AB021861) was subcloned into pGEM-T Easy vector (Promega). For *in situ* hybridisation, skin sections from untreated WT mice were hybridised with digoxigenin-labelled RNA probes at 60°C for 16 h. Bound label was detected using NBT-BCIP, an alkaline phosphate colour substrate. The sections were counterstained with Kernechtrot (MUTO PURE CHEMICALS).

FACS analysis

For measurement of ROS production, HaCaT keratinocytes were pretreated with 2 μM DCHF-DA and then incubated with DMSO or 100 μM DMBA for 30 min. Fluorescence intensity was measured by flow cytometry with an excitation wavelength of 488 nm and emission wavelength of 580 nm. Fluorescent cells were detected by FACScalibar (BD Biosciences) and analysed using FlowJo software (Tree Star).

Immunoblotting

Cells were lysed with a lysis buffer containing 50 mM Tris–HCl, pH 8.0, 150 mM NaCl, 1% deoxycholate, 1% Triton X-100, 10 mM EDTA, 1 mM phenylmethylsulfonyl fluoride and 5 μg/ml aprotinin. Excised mouse skin was lysed in a buffer containing 1% Triton-X, 50 mM HEPES-KOH, pH7.5, 10 mM KCl, 150 mM NaCl, 1 mM EDTA, 1 mM EGTA, 1.5 mM MgCl2 and 10% glycerol supplemented with a phosphatase inhibitor cocktail (PhosSTOP; Roche). Lysates were resolved on SDS–PAGE and electroblotted onto polyvinylidene difluoride membranes. After blocking with 5% skim milk in TBS-T (50 mM Tris–HCl, pH 8.0, 150 mM NaCl and 0.05% Tween 20), the membranes were probed with antibodies. The antibody/antigen complexes were detected using the ECL system (GE Healthcare).

Assessment of cell death of keratinocytes

Induction of death of primary keratinocytes by DMBA was determined using ToxCount (Active Motif) according to the manufacturer's instructions. Briefly, primary keratinocytes were seeded onto glass-bottomed dishes. Cells treated with DMBA were incubated with 0.5 mM calcein AM and 0.5 mM EthD-1 for 30 min at 37°C. Fluorescence images were acquired using an LSM510 laser-scanning unit coupled to an Axiovert 100 M inverted microscope with a C Apochromat × 63 objective lens (Carl Zeiss). DNA fragmentation in primary keratinocytes was quantified using the Cell Death Detection ELISAPLUS Kit (Roche Diagnostics) according to the manufacturer's instructions. The viability of primary keratinocytes treated with UVA was determined using the MTT assay-based Cell Counting Kit-8 (Dojindo) according to the manufacturer's instructions.

TUNEL staining and immunohistochemical staining for active caspase-3

Samples were fixed with Tissue Fixative (Genostaff), embedded in paraffin, and sectioned at 4 μm. Tissue sections were de-paraffined with xylene, and rehydrate through a ethanol series and TBS. After blocking the endogenous peroxidase with 3% H_2O_2 in methanol for 15 min, TUNEL staining was performed using the ApopTag Peroxidase *in situ* Apoptosis Detection Kit (Chemicon, S7100) according to manufacturer's instructions. Peroxidase activity was visualised with diaminobenzidine. The sections were counterstained with Mayer's Hematoxylin (Muto), dehydrated, and then mounted with Malinol (Muto). For active caspase-3 immunostaining, antigen retrieval was performed by microwave treatment in 1 mM EDTA buffer, pH 9.0. Endogenous peroxidase was blocked with 0.3% H_2O_2 in methanol for 30 min, followed by incubation with Protein Block (Dako). The sections were incubated with rabbit polyclonal antibody to Caspase 3 (R&D Systems) at 4°C overnight. After washing with TBS, the sections were treated with the Biotin

blocking system (Dako) and biotin-conjugated goat anti-rabbit Ig (Dako) diluted 1:600 for 30 min at room temperature, followed by addition of peroxidase conjugated streptavidin (Nichirei) for 5 min. Peroxidase activity was visualised with diaminobenzidine. The sections were counterstained with Mayer's Hematoxylin (Muto), dehydrated, and then mounted with Malinol (Muto). For image acquisition, a microscope (DM4000B; Leica) equipped with a digital camera (DC300FX; Leica) was used.

Analysis of expression of ASK2 mRNA in human cancer cell lines

To examine the expression of ASK2 mRNA in human cancer cells (cervical cancer, 10 lines; ovarian cancer, 30 lines; oral cancer, 18 lines; esophageal cancer, 43 lines; gastric cancer, 32 lines; colorectal cancer, 13 lines), quantitative real-time RT–PCR analysis was performed with TaqMan universal PCR master mix using the ABI Prism 7000 Sequence Detection System (Applied Biosystems) according to the manufacturer's instructions. The human GAPDH gene was used as an endogenous control. TaqMan probes and primers for ASK2 (No.Hs00177968_m1) and GAPDH (No.4326317E) were assay-on-demand gene expression products (Applied Biosystems). All samples were tested in duplicate. To normalise the relative expression of ASK2 to the GAPDH control, standard curves were prepared for ASK2 and GAPDH in each experiment.

Histology and immunohistochemistry

Surgically resected specimens were obtained from patients who received esophagectomy to ESCC in the National Defense Medical College Hospital (Saitama, Japan) between 1985 and 2003. Resected tissue specimens were formalin-fixed, paraffin-embedded, and routinely processed for pathological diagnosis. Written consent was acquired from each patient in the formal style, and the local ethics committees approved this study. These tissue blocks were cut into 4-μm thick sections and subjected to immunohistochemistry. Indirect immunohistochemistry of specimens using ASK2 antibody was performed as follows. Briefly, antigens were retrieved by autoclave in citrate buffer (pH 6.0) for 10 min at 120°C. After blocking in 2% normal swine serum, the slides were incubated with 3.5 μg/ml human ASK2 antibody overnight at 4°C, and then reacted with a dextran polymer reagent combined with secondary antibody and peroxidase (Envision Plus; DAKO). Antigen–antibody reactions were visualised with 0.2% diaminobenzidine tetrahydrochloride and hydrogen peroxide. The slides were counterstained with Mayer's hematoxylin. For morphological analysis of the TPA-treated mouse skin, the dorsal skin of WT, *ASK2*$^{-/-}$ and *ASK1*$^{-/-}$ mice was treated twice with acetone or TPA (10 μg each time) with a 24-h interval. Mice were killed at 48 h after the latter treatment. Sections (8 μm) of fresh-frozen TPA-treated skin were stained with hematoxylin and eosin. Images were acquired and processed as described in the section on TUNEL staining and immunohistochemical staining for active caspase-3.

Analysis of expression of cytokine genes in mouse skin

To quantify mRNA expression of TNF-α and IL-6, total RNA was isolated from mouse skin using ISOGEN (Nippon Gene) and reverse-transcribed with the QuantiTect Reverse Transcription Kit. Quantitative reverse-transcription PCR was performed with SYBR Green PCR Master Mix using the ABI PRISM 7000 Sequence Detection System (Applied Biosystems). To normalise the relative expression of TNF-α and IL-6 to the GAPDH control, standard curves were prepared for each gene and GAPDH in each experiment.

Supplementary data

Supplementary data are available at *The EMBO Journal* Online (http://www.embojournal.org).

Acknowledgements

We thank all the members of Cell Signaling Laboratory for critical comments. This study was supported in part by Grants-in-Aid for Scientific Research from the Ministry of Education, Culture, Sports, Science and Technology in Japan, the Takeda Science Foundation and Grant in aid from the Tokyo Biochemical Research Foundation.

References

Agar NS, Halliday GM, Barnetson RS, Ananthaswamy HN, Wheeler M, Jones AM (2004) The basal layer in human squamous tumors harbors more UVA than UVB fingerprint mutations: a role for UVA in human skin carcinogenesis. *Proc Natl Acad Sci USA* **101:** 4954–4959

Ancrile B, Lim KH, Counter CM (2007) Oncogenic Ras-induced secretion of IL6 is required for tumorigenesis. *Genes Dev* **21:** 1714–1719

Azad N, Rojanasakul Y, Vallyathan V (2008) Inflammation and lung cancer: roles of reactive oxygen/nitrogen species. *J Toxicol Environ Health B Crit Rev* **11:** 1–15

Benhar M, Engelberg D, Levitzki A (2002) ROS, stress-activated kinases and stress signaling in cancer. *EMBO Rep* **3:** 420–425

Bode AM, Dong Z (2003) Mitogen-activated protein kinase activation in UV-induced signal transduction. *Sci STKE* **2003:** RE2

Chen N, Nomura M, She QB, Ma WY, Bode AM, Wang L, Flavell RA, Dong Z (2001) Suppression of skin tumorigenesis in c-Jun NH(2)-terminal kinase-2-deficient mice. *Cancer Res* **61:** 3908–3912

Coussens LM, Werb Z (2002) Inflammation and cancer. *Nature* **420:** 860–867

Dolado I, Swat A, Ajenjo N, De Vita G, Cuadrado A, Nebreda AR (2007) p38alpha MAP kinase as a sensor of reactive oxygen species in tumorigenesis. *Cancer Cell* **11:** 191–205

Evan GI, Vousden KH (2001) Proliferation, cell cycle and apoptosis in cancer. *Nature* **411:** 342–348

Frenkel K, Wei L, Wei H (1995) 7,12-dimethylbenz[a]anthracene induces oxidative DNA modification *in vivo*. *Free Radic Biol Med* **19:** 373–380

Fujino G, Noguchi T, Matsuzawa A, Yamauchi S, Saitoh M, Takeda K, Ichijo H (2007) Thioredoxin and TRAF family proteins regulate reactive oxygen species-dependent activation of ASK1 through reciprocal modulation of the N-terminal homophilic interaction of ASK1. *Mol Cell Biol* **27:** 8152–8163

Ha HY, Kim Y, Ryoo ZY, Kim TY (2006) Inhibition of the TPA-induced cutaneous inflammation and hyperplasia by EC-SOD. *Biochem Biophys Res Commun* **348:** 450–458

Han J, Sun P (2007) The pathways to tumor suppression via route p38. *Trends Biochem Sci* **32:** 364–371,

Hsu TC, Young MR, Cmarik J, Colburn NH (2000) Activator protein 1 (AP-1)- and nuclear factor kappaB (NF-kappaB)-dependent transcriptional events in carcinogenesis. *Free Radic Biol Med* **28:** 1338–1348

Hui L, Bakiri L, Mairhorfer A, Schweifer N, Haslinger C, Kenner L, Komnenovic V, Scheuch H, Beug H, Wagner EF (2007) p38alpha suppresses normal and cancer cell proliferation by antagonizing the JNK-c-Jun pathway. *Nat Genet* **39:** 741–749

Ichijo H, Nishida E, Irie K, ten Dijke P, Saitoh M, Moriguchi T, Takagi M, Matsumoto K, Miyazono K, Gotoh Y (1997) Induction of apoptosis by ASK1, a mammalian MAPKKK that activates SAPK/JNK and p38 signaling pathways. *Science* **275:** 90–94

Kaghad M, Bonnet H, Yang A, Creancier L, Biscan JC, Valent A, Minty A, Chalon P, Lelias JM, Dumont X, Ferrara P, McKeon F, Caput D (1997) Monoallelically expressed gene related to p53 at 1p36, a region frequently deleted in neuroblastoma and other human cancers. *Cell* **90:** 809–819

Kyriakis JM, Avruch J (2001) Mammalian mitogen-activated protein kinase signal transduction pathways activated by stress and inflammation. *Physiol Rev* **81:** 807–869

Liu J, Lin A (2005) Role of JNK activation in apoptosis: a double-edged sword. *Cell Res* **15:** 36–42

Marnett LJ (2000) Oxyradicals and DNA damage. *Carcinogenesis* **21:** 361–370

Matsuzawa A, Saegusa K, Noguchi T, Sadamitsu C, Nishitoh H, Nagai S, Koyasu S, Matsumoto K, Takeda K, Ichijo H (2005) ROS-dependent activation of the TRAF6-ASK1-p38 pathway is selectively required for TLR4-mediated innate immunity. *Nat Immunol* **6:** 587–592

Moore RJ, Owens DM, Stamp G, Arnott C, Burke F, East N, Holdsworth H, Turner L, Rollins B, Pasparakis M, Kollias G, Balkwill F (1999) Mice deficient in tumor necrosis factor-alpha are resistant to skin carcinogenesis. *Nat Med* **5:** 828–831

Mueller MM (2006) Inflammation in epithelial skin tumours: old stories and new ideas. *Eur J Cancer* **42:** 735–744

Muqbil I, Azmi AS, Banu N (2006) Prior exposure to restraint stress enhances 7,12-dimethylbenz(a)anthracene (DMBA) induced DNA damage in rats. *FEBS Lett* **580:** 3995–3999

Murakami S, Noguchi T, Takeda K, Ichijo H (2007) Stress signaling in cancer. *Cancer Sci* **98:** 1521–1527

Nakamura Y, Murakami A, Ohto Y, Torikai K, Tanaka T, Ohigashi H (1998) Suppression of tumor promoter-induced oxidative stress and inflammatory responses in mouse skin by a superoxide generation inhibitor 1′-acetoxychavicol acetate. *Cancer Res* **58:** 4832–4839

Noguchi T, Takeda K, Matsuzawa A, Saegusa K, Nakano H, Gohda J, Inoue JI, Ichijo H (2005) Recruitment of tumor necrosis factor receptor-associated factor family proteins to apoptosis signal-regulating kinase 1 signalosome is essential for oxidative stress-induced cell death. *J Biol Chem* **280:** 37033–37040

O'Neill LA (2006) Targeting signal transduction as a strategy to treat inflammatory diseases. *Nat Rev Drug Discov* **5:** 549–563

Roessner A, Kuester D, Malfertheiner P, Schneider-Stock R (2008) Oxidative stress in ulcerative colitis-associated carcinogenesis. *Pathol Res Pract* **204:** 511–524

Saitoh M, Nishitoh H, Fujii M, Takeda K, Tobiume K, Sawada Y, Kawabata M, Miyazono K, Ichijo H (1998) Mammalian thioredoxin is a direct inhibitor of apoptosis signal-regulating kinase (ASK) 1. *EMBO J* **17:** 2596–2606

Suganuma M, Okabe S, Marino MW, Sakai A, Sueoka E, Fujiki H (1999) Essential role of tumor necrosis factor alpha (TNF-alpha) in tumor promotion as revealed by TNF-alpha-deficient mice. *Cancer Res* **59:** 4516–4518

Sumbayev VV, Yasinska IM (2005) Regulation of MAP kinase-dependent apoptotic pathway: implication of reactive oxygen and nitrogen species. *Arch Biochem Biophys* **436:** 406–412

Sun P, Yoshizuka N, New L, Moser BA, Li Y, Liao R, Xie C, Chen J, Deng Q, Yamout M, Dong MQ, Frangou CG, Yates W, Pe H (2007) PRAK is essential for ras-induced senescence and tumor suppression. *Cell* **128:** 295–308

Takeda K, Noguchi T, Naguro I, Ichijo H (2008) Apoptosis signal-regulating kinase 1 in stress and immune response. *Annu Rev Pharmacol Toxicol* **48:** 199–225

Takeda K, Shimozono R, Noguchi T, Umeda T, Morimoto Y, Naguro I, Tobiume K, Saitoh M, Matsuzawa A, Ichijo H (2007) Apoptosis signal-regulating kinase (ASK) 2 functions as a mitogen-activated protein kinase kinase kinase in a heteromeric complex with ASK1. *J Biol Chem* **282:** 7522–7531

Tobiume K, Matsuzawa A, Takahashi T, Nishitoh H, Morita K, Takeda K, Minowa O, Miyazono K, Noda T, Ichijo H (2001) ASK1 is required for sustained activations of JNK/p38 MAP kinases and apoptosis. *EMBO Rep* **2:** 222–228

Tobiume K, Saitoh M, Ichijo H (2002) Activation of apoptosis signal-regulating kinase 1 by the stress-induced activating phosphorylation of pre-formed oligomer. *J Cell Physiol* **191:** 95–104

Valencia A, Kochevar IE (2006) Ultraviolet A induces apoptosis via reactive oxygen species in a model for Smith-Lemli-Opitz syndrome. *Free Radic Biol Med* **40:** 641–650

Ventura JJ, Tenbaum S, Perdiguero E, Huth M, Guerra C, Barbacid M, Pasparakis M, Nebreda AR (2007) p38alpha MAP kinase is essential in lung stem and progenitor cell proliferation and differentiation. *Nat Genet* **39:** 750–758

Zarubin T, Han J (2005) Activation and signaling of the p38 MAP kinase pathway. *Cell Res* **15:** 11–18

J Gastroenterol 2009; 44:13–25
DOI 10.1007/s00535-008-2291-5

Journal of Gastroenterology

Review

Narrow-band imaging of the gastrointestinal tract

Manabu Muto, Takahiro Horimatsu, Yasumasa Ezoe, Kimiko Hori, Yoshiyuki Yukawa, Shuko Morita, Shinichi Miyamoto, and Tsutomu Chiba

Department of Gastroenterology and Hepatology, Kyoto University Graduate School of Medicine, 54 Shogoin Kawaracho, Sakyo-ku, Kyoto 606-8507, Japan

Key words: narrow-band imaging, GI tract, early detection, diagnosis

Introduction

A narrow-band imaging (NBI) system is now commercially available worldwide from Olympus Medical Systems as an endoscopic diagnostic tool for the gastrointestinal (GI) tract. The most important strengths of the NBI system are enhancements in endoscopic visualization of superficial neoplastic lesions and the microvascular architecture.[1–5] As endoscopic magnification maximizes the latter strength, NBI is expected to yield breakthroughs in endoscopic diagnosis. Angiogenesis is critical in the transition from the premalignant to the malignant phenotype, so detection and diagnosis based in part on morphologic changes to the microvessels are ideal. These advantages will potentially allow us to easily identify and accurately diagnose superficial neoplasms of the GI tract.

In contrast, conventional endoscopic diagnosis using white light is based on subtle morphological changes such as superficially elevated, flat, or depressed lesions and on minimal changes in color such as reddish discoloration. However, these findings are difficult to recognize, especially for inexperienced endoscopists, who require much skill training. As a result, the diagnosis may be inaccurate or a precancerous lesion or superficial cancer in the GI tract may be overlooked. From the point of view of the effective cancer screening, these disadvantages must be overcome.

When combined with magnifying endoscopy, NBI can clearly demarcate the margin between a nonneoplastic lesion and a cancerous lesion and can increase the contrast of morphological changes of the mucosal surface and microvessels. Inoue and colleagues[6,7] and Yao and colleagues[8,9] have already reported the importance of findings of microvascular irregularities in cancer of the esophagus and stomach, respectively. However, in images magnified while using white light, these changes have been difficult to identify. With NBI, these changes are easily recognized, thus renewing our awareness of the importance of microvascular irregularities in cancerous lesions.

Herein, we review publications on use of an NBI system in the GI tract.

Technical background of NBI

The NBI system was developed through collaboration between Japanese National Cancer Center Hospital East and Olympus Medical Systems (Tokyo, Japan) with support since 1999 by a Grant for Scientific Research Expenses for Health and Welfare Programs. Sano et al.[10] first reported the clinical utility of NBI in the GI tract in 2001. After respective approval by the U.S. Food and Drug Administration and the Japanese Ministry of Health, Labour and Welfare, Olympus Medical Systems introduced the NBI system commercially in the United States, in December 2005, and Japan, in May 2006.

There are two types of videoendoscope system: a red-green-blue (RGB) sequential illumination type and a color chip type. An RGB sequential illumination system uses three broadband optical filters that cover all wavelengths of the visible spectrum, approximately from 400 to 800 nm (Fig. 1A). A color chip system uses a color charge-coupled device (CCD) chip with tiny color filters in each pixel (Fig. 2A). Both systems use a xenon lamp as the light source. The difference between these two systems is in how the color image is created. The NBI system uses an NBI filter to create two narrow-band

Received: August 14, 2008 / Accepted: August 18, 2008
Reprint requests to: M. Muto

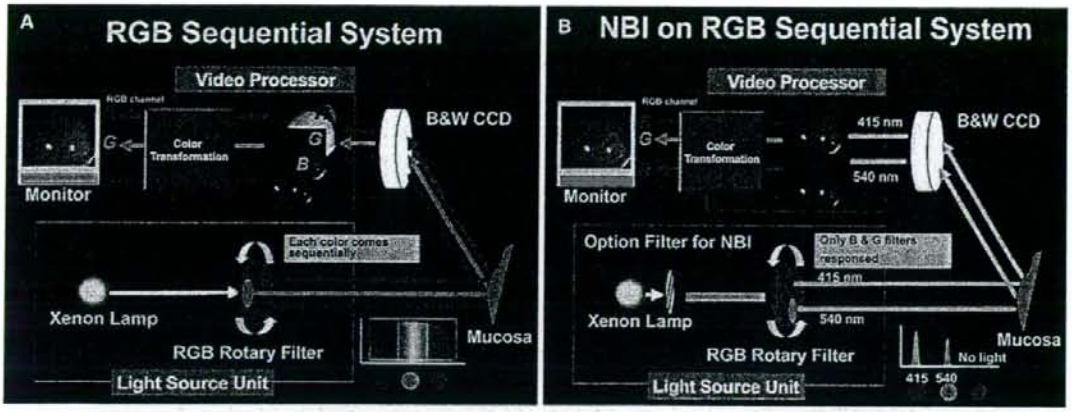

Fig. 1. **A** The red-green-blue (*RGB*) sequential illumination system. **B** A narrow-band imaging (*NBI*) system based on the RGB sequential illumination system. The NBI system uses two narrow-band illumination beams of 415 and 540 nm produced by an NBI filter

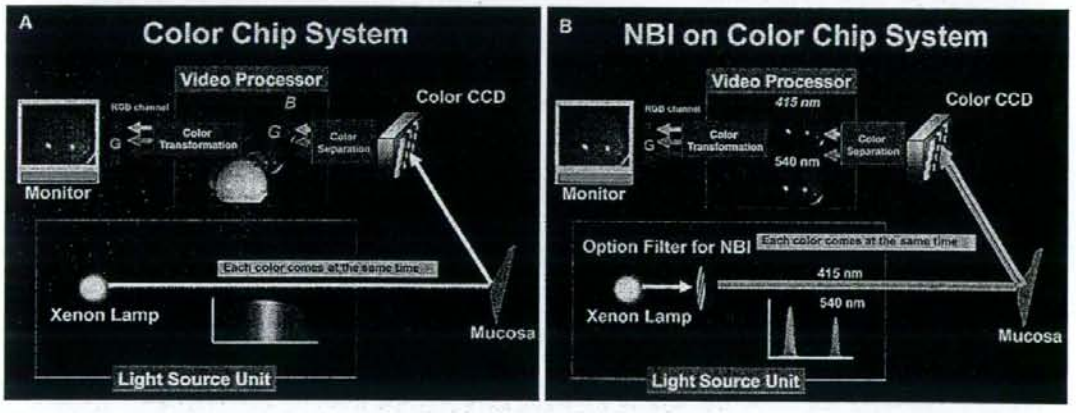

Fig. 2. **A** The color chip system uses a color charge-coupled device (*CCD*) chip. **B** The NBI system based on color chip system. The NBI system uses two narrow-band illumination beams of 415 and 540 nm produce by an NBI filter

illumination beams at 415 and 540 nm (Figs. 1B, 2B). Under NBI observation, the broadband white light derived from the xenon lamp is split into two bands (wavelengths, 415 and 540 nm), which illuminate the surface of the mucosa.

In NBI with the RGB sequential illumination system, the NBI filter is placed in the light path in front of an RGB rotary filter (Fig. 1B). In observations with the NBI filter, the illumination passes only the B and G filters to obtain images at 415 and 540 nm. For NBI observation with the color chip system (Fig. 2B), the NBI filter is placed in the light path, whereas this filter is not used for conventional white light observation. Two narrow-band images at 415 and 540 nm should be produced when the NBI filter is used. However, to create a color image on a CRT or liquid crystal monitor, three images are needed to be output to its R, B, and G channels. Thus, the 415-nm beam is allocated to the B and G channels so that the blood vessels on the mucosal surface are reproduced with a brownish color, and the 540-nm beam is allocated to the R channel so that the vessels in the deeper layer are indicated by cyan.

Combination with magnifying endoscopy

NBI performance is maximized, increasing the accuracy of the diagnosis, when it is combined with magnifica-

tion. However, the capabilities of the RGB sequential illumination system and those of the color CCD system to utilize magnification differ. While the RGB sequential illumination system allows for optical magnification of the image by up to 80 times, the color CCD system has a digital zoom for 1.2 × and 1.5 × magnification. Thus, the diagnostic power of these two systems is likely to differ. In addition, NBI observation without magnification has a potential disadvantage because the image may be too dark to identify morphological and color changes.

Image-enhanced endoscopy

Recently, the American Gastroenterological Association proposed the term "image enhanced endoscopy" (IEE),[11] which encompasses various means of enhancing contrast during endoscopy, by using dye, optical, or electronic methods. IEE includes both dye-based and equipment-based methods, and the NBI system is classified as optical equipment-based IEE.

Squamous cell carcinoma (oropharynx, hypopharynx, and esophagus)

Major histological types of esophageal cancer are squamous cell carcinoma (SCC) and adenocarcinoma. The former is mainly associated with alcohol and tobacco abuse, and the latter is associated with acid reflux. Lugol chromoendoscopy is the standard technique for detecting early SCC in the esophagus.[12] While normal epithelium is stained dark brown by the Lugol solution, a cancerous lesion remains unstained and is pink under white light observation.[13] However, Lugol solution is irritating and causes unpleasant reactions such as chest pain and discomfort and sometimes allergic shock. In addition, Lugol dye solution cannot be applied to the oropharyngeal or hypopharyngeal mucosa because of aspiration risk. Therefore, early detection of SCC in this region is quite difficult, and most SCCs are diagnosed at an advanced stage, leading to a poor prognosis.

Morphological changes to an intrapapillary capillary loop (IPCL) have been recognized as a new target for diagnosis of SCC in the esophagus.[6,7] However, evaluation of IPCLs under white light observation requires high levels of proficiency. Yoshida et al.[14] compared the ability of experienced endoscopists and novices to identify and evaluate IPCLs by NBI and white light observation. Both experienced and novice assessors reported that image contrast was superior and identification and evaluation of IPCLs were easier with NBI than with white light observation. Furthermore, NBI with magnification improved the diagnostic accuracy of depth of invasion based on IPCL findings, especially for inexperienced endoscopists. Clinically, it is very important to shorten the learning curve of the inexperienced endoscopist.

Muto et al.[4,15] reported that NBI combined with magnifying endoscopy is very useful for identifying superficial SCC in the head and neck region. They also reported that visualization of cancerous lesions and abnormal microvessels is significantly improved by NBI compared with white light observation because of enhancement of microvascular architecture.[3,4] This finding is clinically significant because no cases of superficial cancer in the oropharynx or hypopharynx were reported before the advent of NBI.

Early detection enables us to apply endoscopic mucosal resection (EMR) and endoscopic subepithelial dissection (ESD) methods in the head and neck region as well as in the GI tract.[15] This benefits the patient greatly because organs and functions can be preserved by a less-invasive treatment, and it may even save the patient's life.

The usefulness of NBI has also been confirmed in the ear-nose-throat (ENT) field. Watanabe et al.[16,17] reported that an NBI rhinolaryngoscope (ENF-V2, Olympus Medical Systems) with a light source (CLV-160B, Olympus Medical Systems) improved the diagnostic accuracy and negative predictive value of superficial lesions in the oropharynx and hypopharynx. According to the concept of "field cancerization," patients with head and neck cancer or esophageal SCC have a high risk of development of synchronous or metachronous SCC in these regions. Because NBI is expected to detect cancer at an earlier stage, it will contribute to the improved survival of patients with multiple SCCs.

Preliminary results of a Japanese multicenter prospective randomized controlled study comparing detection and diagnostic accuracy of superficial SCC in the head and neck region and the esophagus between NBI and conventional white light observation, conducted in a back-to-back fashion, showed a significantly higher detection rate and accuracy with NBI.[18] This result suggests that NBI should be a standard examination in screening for cancer of the squamous epithelium.

Table 1 summarizes data for NBI for the esophagus and the head and neck region. All of the studies in the GI field were performed using an RGB sequential illumination endoscopy system. In contrast, endoscopy of the ENT field was conducted using the color CCD chip system. However, the results obtained using both systems demonstrated that NBI could detect early cancer both in the esophagus and in the head and neck region.